Electronic Supplementary Material (ESI) for Physical Chemistry Chemical Physics.

Glucose transport via the Pseudomonads porin OprB. Implications for the design of Trojan-horse antibiotics

Joan Coines,[1] Silvia Acosta-Gutierrez,[2] Igor Bodrenko,[2] Carme Rovira,[1,3] and Matteo Ceccarelli[2,4*]

[1] Departament de Química Inorgànica i Orgànica and Institut de Quiímica Teòrica i Computacional (IQTCUB), Universitat de Barcelona, Martí i Franquès 1, 08028 Barcelona, Spain. [2] Department of Physics, University of Cagliari, Cittadella Universitaria di Monserrato, S.P.8−km 0.700, 09042 Monserrato, Cagliari, Italy. [3] Institució Catalana de Recerca i Estudis Avançats (ICREA), Passeig Lluís Companys 23, 08018, Barcelona, Spain. [4] CNR-IOM Unita di Cagliari, Moserrato, Italy

SAG present address: Department of Chemistry, University College London, London, UK.

CONTENTS

1. OprB equilibration

The OprB porin was equilibrated at 300 K during 4 ns in the NPT ensemble (Berendsen barostat) and then 100 ns in the NVT ensemble (Langevin thermostat), considering a cell dimension of 77.75 × 77.75 × 102.17 $Å^3$. The equilibration protocol used was the following.

1. 200 steps of conjugate-gradient minimization.
2. 5 ps at 10 K in the NVT ensemble, cell dimensions: 85 × 85 x 109 $Å^3$.
3. 50 ps at 100 K in the NPT ensemble.
4. 100 ps at 200 K in the NPT ensemble.
5. 200 ps at 250 K in the NPT ensemble.
6. 200 ps at 300 K in the NPT ensemble.
7. 1000 ps at 300 K in the NPT ensemble.
8. 500 ps at 300 K in the NPT ensemble.
9. 2000 ps at 300 K in the NPT ensemble.
10. 100 ns at 300 K in the NVT ensemble, cell dimensions: 77.75 × 77.75 × 102.17 $Å^3$.

During steps 1-5, restraints of 10 kcal/mol were applied to C_α and C_β atoms of the protein backbone, and to the phosphorus atom of POPC residues. At steps 6-8, only the restraint to C_α and C_β atoms was maintained.

In the NPT ensemble, the Berendsen barostat was employed. During steps 3-6 and 8, the ratio of the X-Y dimensions was kept constant.

For steps 1-4, the timestep and the hydrogen scale were set at 1. Then, from the steps 5 to 8, the timestep and the hydrogen scale were set at 2 and 1, respectively. After that, the hydrogen scale was increased to 2 at step 9. Finally, at step 10 these parameters were increased to 4.

During the equilibration several properties have been monitored (cell dimension, RMSD and RMSF), paying attention to L2 and L3 loops (Figure S2-S4). In the NPT ensemble, as the pressure is constant, the cell dimension (i.e., volume) fluctuates.

2. OprB production

After the equilibration (previous section), 1 μs of molecular dynamics (production run) has been performed to analyze dynamical properties.

The average area per lipid for the top and bottom leaflets are 62.21 ± 0.94 $Å^2$ and 60.97 ± 1.79 $Å^2$ respectively. We used GridMAT-MD[1] to calculate the area per lipid from 100 frames obtained along the production run. In this case the area per lipid is not

homogeneous due to the presence of the protein but the results are in good agreement with experimental data in the regions not affected by the protein.[2]

RMSD and RMSF are shown in Figures S5 and S6, respectively.

Starting from the final structure of the production calculation, we have run 4 replicas of 200 ns at 1 M concentration of KCl. From these simulations, we have calculated the ion density of K^+ and Cl^- in order to extract the free energy (Figure 2c in the main text).

3. Charge along Z axis of OprB pore analysis

From the OprB X-ray structure (PDB entry 4GEY), the charge along the Z axis has been computed considering the point charges for every atom from the forcefield. Since electrostatics might be more important in the center of the channel, several radii have been tested. The constriction region is clearly negatively charged (Figure S7).

4. Metadynamics details and convergence analysis

Regarding the metadynamics simulations, multiple-walkers[3] and well-tempered[4] approaches were used in order to accelerate the sampling and obtain a more converged free energy surface (FES), respectively.

The height of the Gaussian terms was set 1 kcal/mol; and their width was set at 0.30 and 0.10 Å for CV_1 and CV_2, respectively. A Gaussian function was deposited every 10 ps of simulation. The temperature was set at 300 K and the bias factor at 10.

The convergence of the multiple-walkers metadynamics simulations employing two collective variables (CV_1 and CV_2, Figure S8) has been tested. During the deposition of the Gaussian terms, the energetic difference between two isoenergetic points from the obtained FES only considering CV_1 (i.e., the one-dimension FES), has been calculated (Figure S9). These points were Z = -45 Å and Z = 45 Å. The simulation was considered converged once several crossing events took place and the aforementioned energetic difference is near zero. The evolution of this CV has been monitored during the metadynamics simulation (Figure S10).

We also investigated the energetics for glucuronate transport through OprB, a substrate supposed not optimal. By using metadynamics we reconstructed the free energy after a single passage through the central region, comparing it with the single passage of glucose. For glucuronate the simulation with a very low deposition time lasted 1.35 μs vs 800 ns for glucose. The comparison with glucose (Figure S11) shows a large difference in the free energy barrier for glucuronate to overcome the central region, 20

kcal/mol vs 5 kcal/mol, in agreement with the measured low rate of swelling for glucuronate with respect to glucose. This energy difference is due to the negative charge of glucuronate, not optimal for the central region that has a few negative residues.

5. Calculation of the molecular flux

Provided the substrate particles are added at molar concentration c to only one side (either *cis* or *trans*) of the channel, the diffusion current through the pore may be calculated using the steady-state solution to the 1D Slomuchowski equation,[5]

$$I_D(c) = Pn_l(c), \quad (1)$$

Where $n_l(c) = SN_A c$ is the linear particle concentration at the entrance to the channel, S is the active surface of the pore (estimated by using a radius of 1.4 nm for OprB), $N_A$is the Avogadro constant and

$$P = \left(\int_0^L \frac{exp\left(\frac{U(Z)}{kT}\right)}{D(Z)} dZ \right)^{-1}, \quad (2)$$

is the permeability coefficient with kT the thermal energy (here T = 300K). The permeability coefficient is calculated by using the using the 1D profile of the potential of mean force obtained from metadynamics, $U(Z)$ (assuming that $U(0) = U(Z) = 0$), and that of the diffusion coefficient, $D(Z)$, along the channel having total length L. For the calculation we assumed a diffusion constant equal for both molecules (D=0.67 nm^2/ns), being structurally similar. The diffusion current is linear with the particle concentration and does not depend on the side of addition of the particles. The total average number of the diffusing particles in the channel reads

$$N_C(c) = n_l(c) \int_0^L exp\left(-\frac{U(Z)}{kT}\right) \left(1 - P \int_0^Z \frac{exp\left(\frac{U(x)}{kT}\right)}{D(x)} dx\right) dZ \quad (3)$$

At small concentration, when $N_C(c) \ll 1$, this quantity has the meaning of the probability to find a particle in the channel. This latter interpretation allows one to bridge the diffusion-scale model with the 2-state Markov model of the particle-pore kinetics.[6] The 2-state Markov model assumes that only one particle at a time may occupy the channel and can describe both the linearity with the concentration and the

saturated behavior of the particle translocation regime. The current from *cis* to *trans* reads

$$I_{C\to T}(c) = \frac{I_D(c)}{N_C(c)+1}, \quad (4)$$

6. References

1 D. R. B. William J. Allen, Justin A. Lemkul, *J. Comput. Chem.*, 2009, **30**, 1952–1958.

2 N. Kučerka, M. P. Nieh and J. Katsaras, *Biochim. Biophys. Acta - Biomembr.*, 2011, **1808**, 2761–2771.

3 P. Raiteri, A. Laio, F. L. Gervasio, C. Micheletti and M. Parrinello, *J. Phys. Chem. B*, 2006, **110**, 3533–3539.

4 A. Barducci, G. Bussi and M. Parrinello, *Phys. Rev. Lett.*, 2008, **100**, 1–4.

5 H. A. Kramers, *Physica*, 1940, **7**, 284–304.

6 D. Colquhoun and A. G. Hawkes, *Proc. R. Soc. London - Biol. Sci.*, 1977, **199**, 231–262.

7. Figures S1-S11

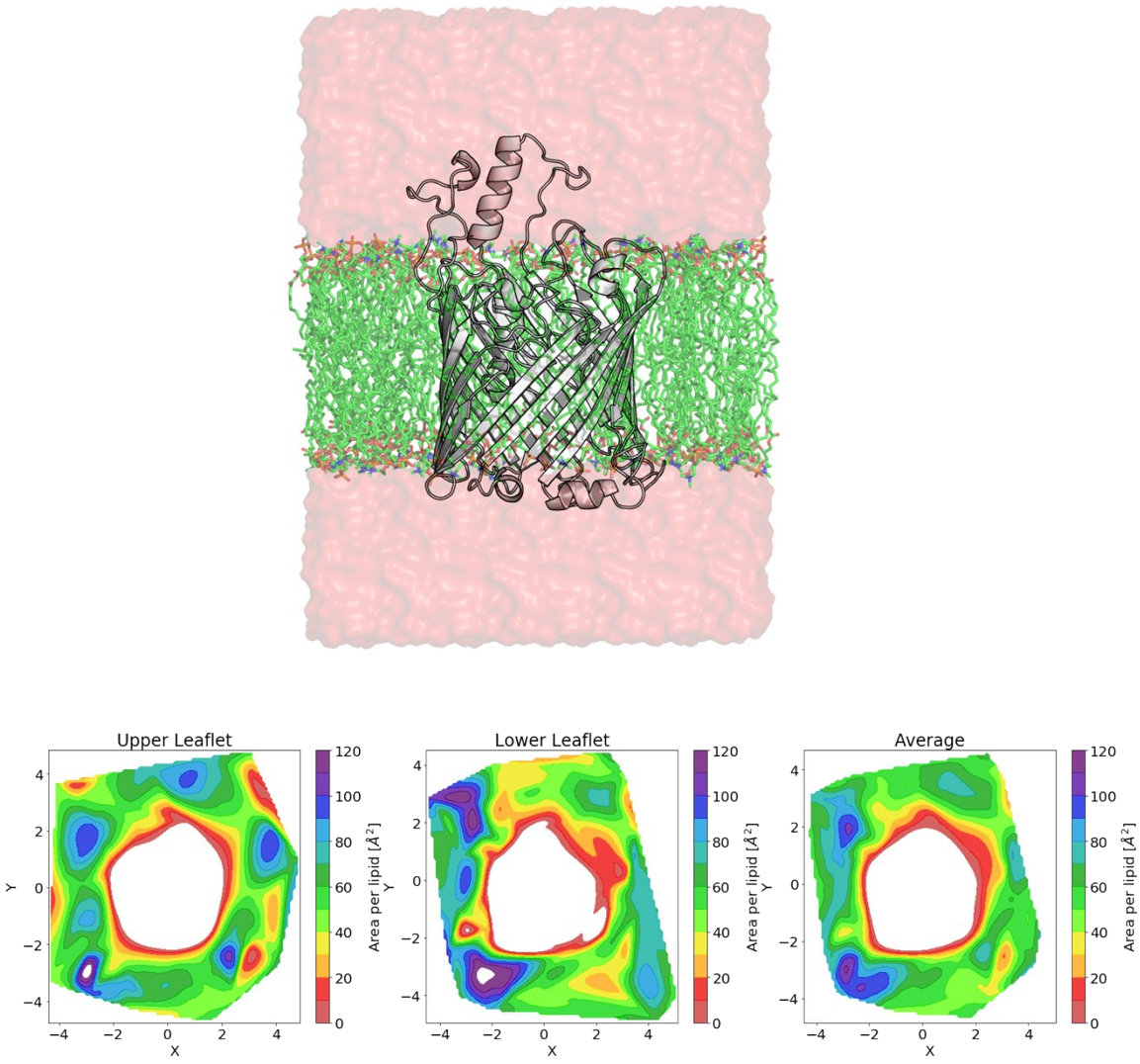

Figure S1. Top: Representation of the system studied in this work, periodically repeated in space. OprB protein is shown in cartoon (grey), PPC lipids in sticks (carbon atoms in color green) and the water solvent in surface representation (red). Bottom: Average area per lipid projected for each lipid onto its average x-y position during simulation for the upper leaflet, lower leaflet and both leaflets average.

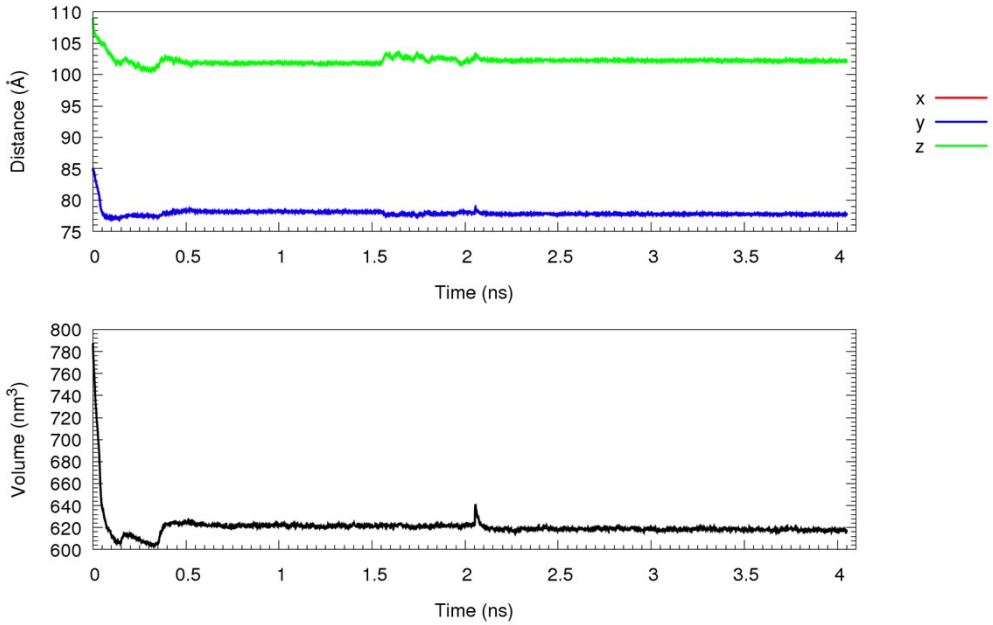

Figure S2. Cell dimension evolution during the NVT equilibration. Cartesian coordinates (top) and volume (bottom).

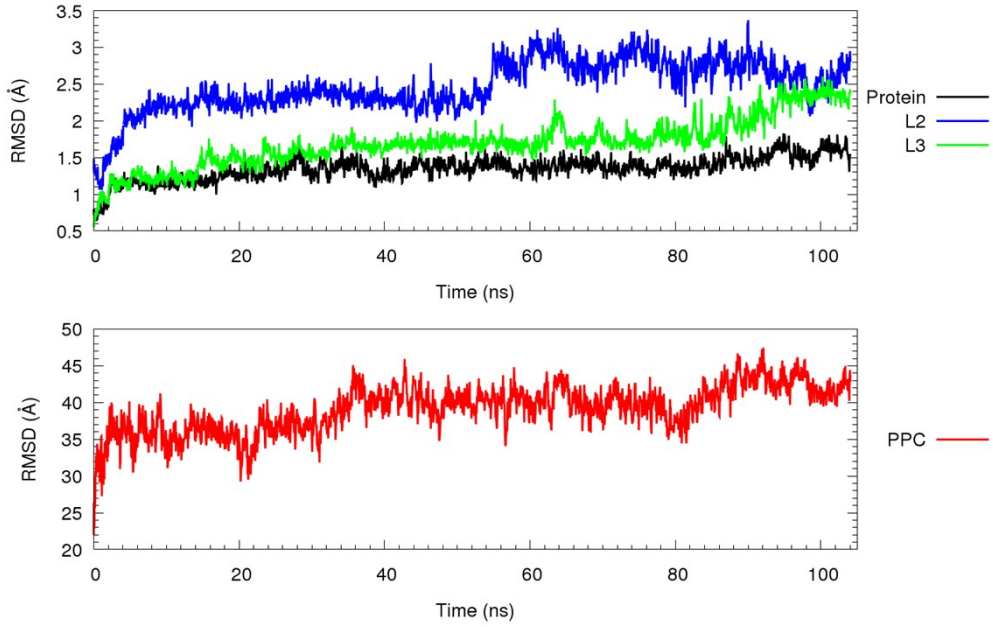

Figure S3. RMSD (Å) of the protein backbone (top) and the phospholipid (bottom) during the equilibration.

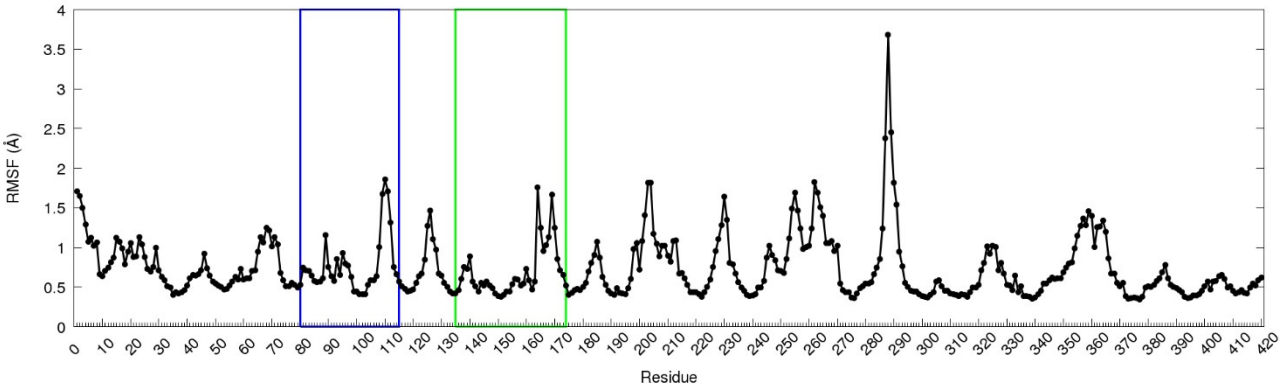

Figure S4. RMSF (Å) of the protein during the equilibration. L2 and L3 loops are shown in blue and green, respectively.

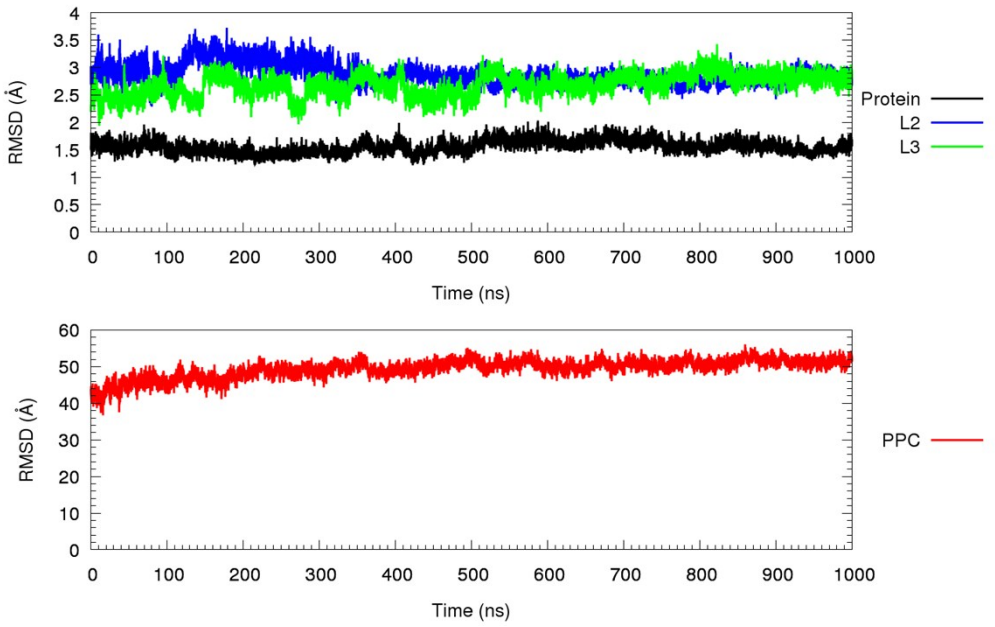

Figure S5. RMSD (Å) of the protein backbone (top) and the phospholipid (bottom) during the production run (1 μs).

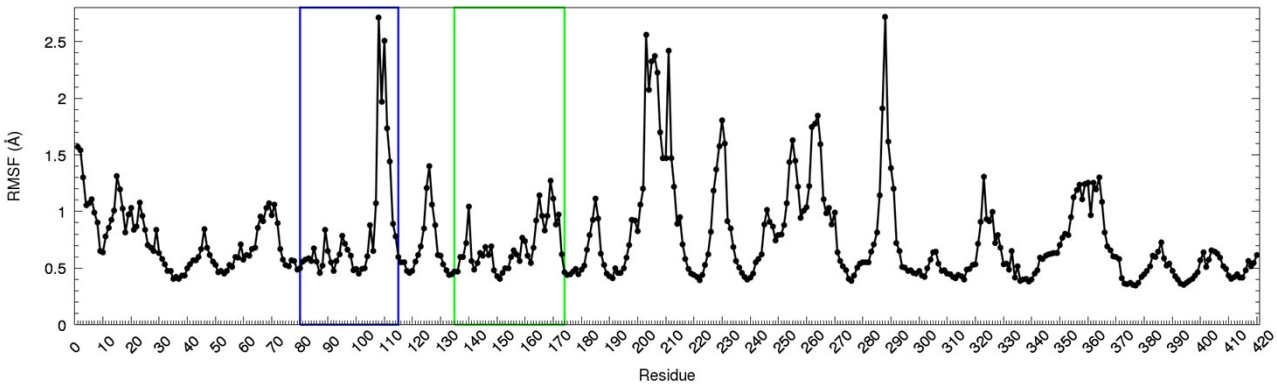

Figure S6. RMSF (Å) of the protein during the production run. L2 and L3 loops are shown in blue and green, respectively.

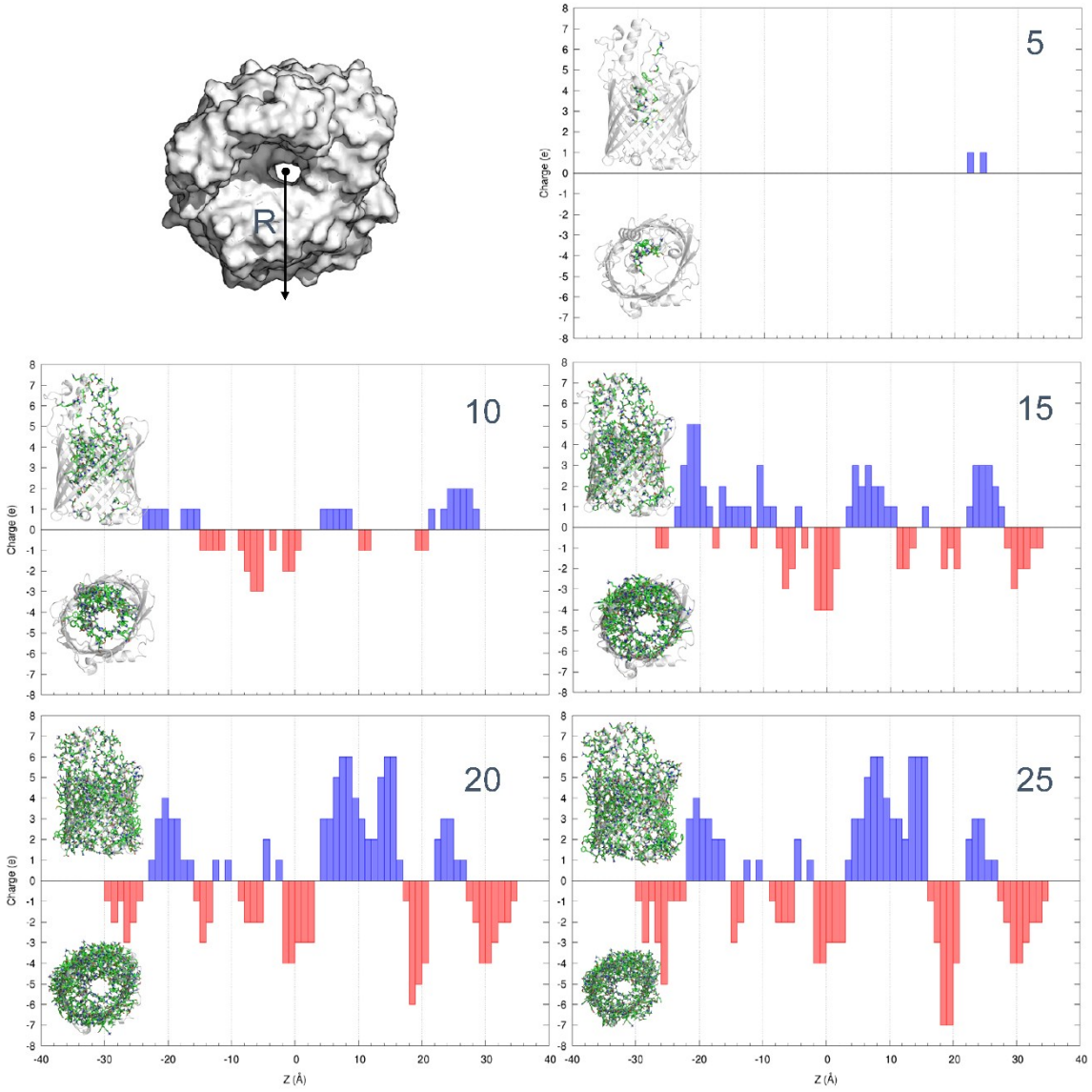

Figure S7. Pore charge across the pore considering the residues located at radius 5, 10, 15, 20 and 25 Å.

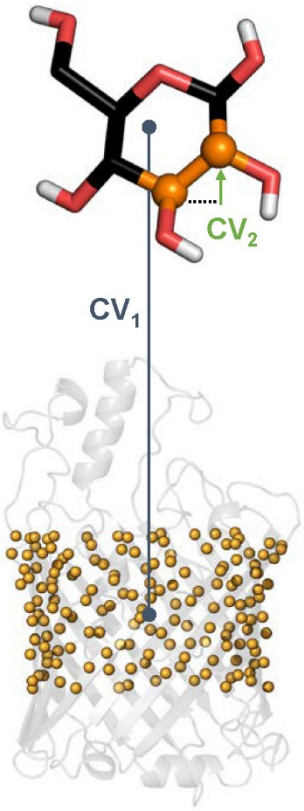

Figure S8. Representation of the collective variables (CVs) employed in this work. CV_1 is defined as the Z component of the distance between the centers of mass of the heteroatoms of the substrate and the C_α atoms of the β-barrel of OprB. CV_2 is defined as the Z component of the distance between C2 and C3 atoms of the substrate.

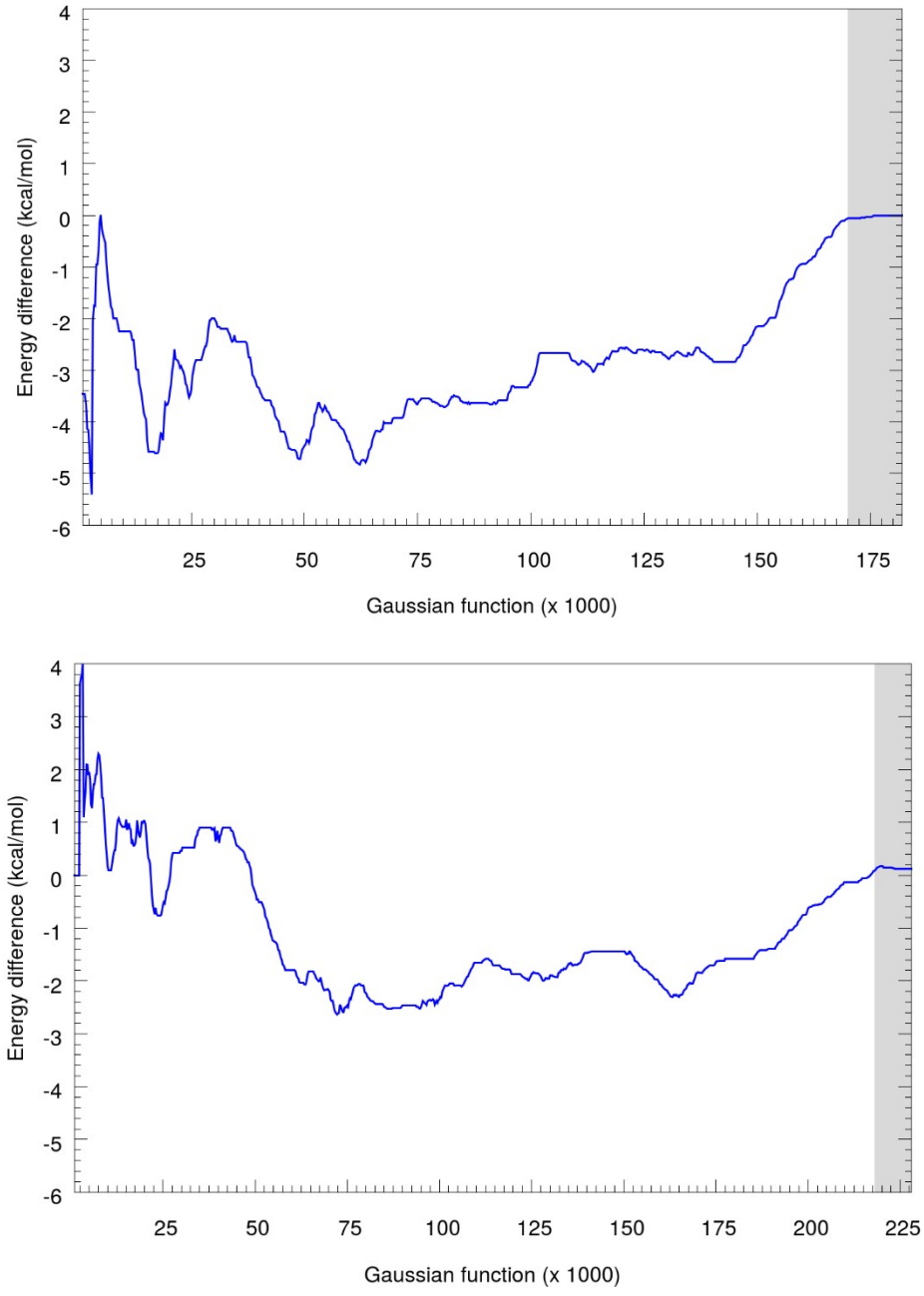

Figure S9. Free energy difference between Z = -45 Å and Z = 45 Å, when the FES is projected on CV_2 (i.e., only considering CV_1 and the corresponding mono-dimensional FES) during the Gaussian deposition in glucose (top) and DNJ-NAc (bottom) metadynamics.

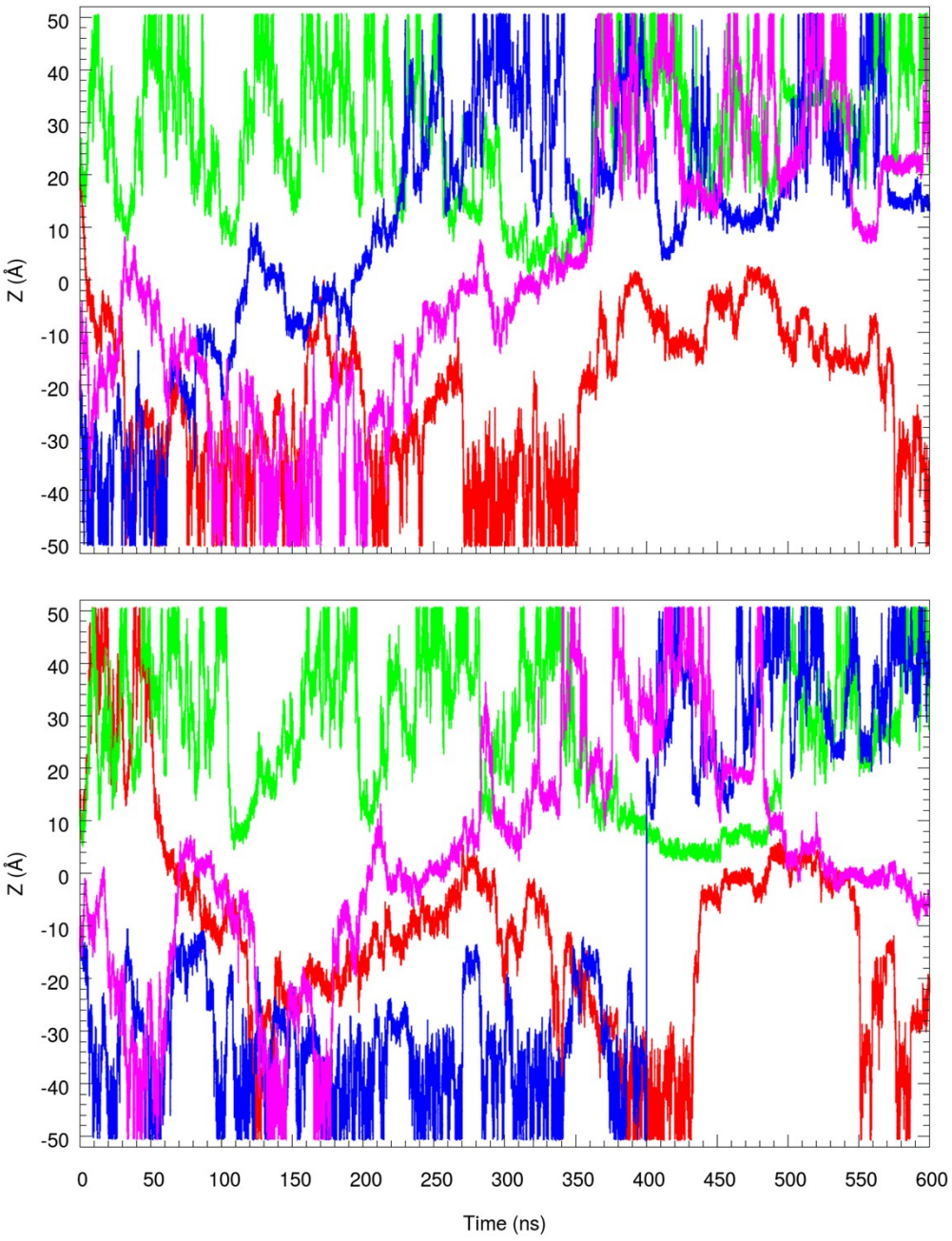

Figure S10. Evolution of CV1 for each walker during the metadynamics simulation of glucose (top) and DNJ-NAc (bottom).

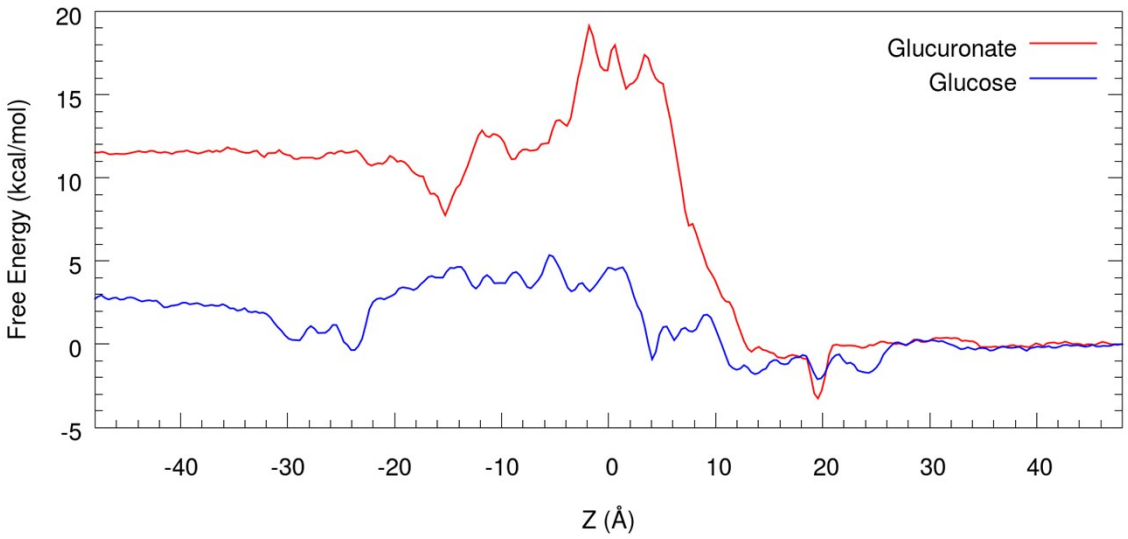

Figure S11. One dimensional free energy reconstructed from a single passage metadynamics simulations of glucuronate and glucose transport through OprB.